



# Gene expression and regulatory factors of the mechanistic target of rapamycin (mTOR) complex 1 predict mammalian longevity

Natalia Mota-Martorell · Mariona Jove · Irene Pradas · Rebeca Berdún · Isabel Sanchez · Alba Naudi · Eloi Gari · Gustavo Barja · Reinald Pamplona

Received: 9 January 2020 / Accepted: 1 June 2020 / Published online: 23 June 2020  
© American Aging Association 2020

**Abstract** Species longevity varies significantly across animal species, but the underlying molecular mechanisms remain poorly understood. Recent studies and omics approaches suggest that phenotypic traits of longevity could converge in the mammalian target of rapamycin (mTOR) signalling pathway. The present study focuses on the comparative approach in heart tissue from 8 mammalian species with a ML ranging from 3.5 to 46 years. Gene expression, protein content, and concentration of regulatory metabolites of the mTOR complex 1 (mTORC1) were measured using

droplet digital PCR, western blot, and mass spectrometry, respectively. Our results demonstrate (1) the existence of differences in species-specific gene expression and protein content of mTORC1, (2) that the achievement of a high longevity phenotype correlates with decreased and inhibited mTORC1, (3) a decreased content of mTORC1 activators in long-lived animals, and (4) that these differences are independent of phylogeny. Our findings, taken together, support an important role for mTORC1 downregulation in the evolution of long-lived mammals.

**Electronic supplementary material** The online version of this article (<https://doi.org/10.1007/s11357-020-00210-3>) contains supplementary material, which is available to authorized users.

**Keywords** Arginine · FKBP12 · Methionine cycle metabolites · mTOR · PRAS40 · Raptor

N. Mota-Martorell · M. Jove · I. Pradas · R. Berdún · A. Naudi · R. Pamplona (✉)  
Department of Experimental Medicine, University of Lleida-Lleida Biomedical Research Institute (UdL-IRBLleida), 25198 Lleida, Catalonia, Spain  
e-mail: reinald.pamplona@mex.udl.cat

I. Sanchez  
Proteomics and Genomics Unit, University of Lleida, 25198 Lleida, Catalonia, Spain

E. Gari  
Department of Basic Medical Sciences, University of Lleida-Lleida Biomedical Research Institute (UdL-IRBLleida), 25198 Lleida, Catalonia, Spain

G. Barja (✉)  
Department of Genetics, Physiology and Microbiology, Complutense University of Madrid (UCM), 28040 Madrid, Spain  
e-mail: gbarja@bio.ucm.es

## Introduction

Maximum longevity ('longevity' from here on out) is a species-specific trait that differ more than 75,000-fold among animal species, and more than 200-fold among mammals (Ma and Gladyshev 2017). The longevity of animal species is an endogenous genetically determined adaptation (Libertini 1988; Barja et al. 1994; Skulachev 1997; Bowles 1998; Longo et al. 2005; Barja 2010, 2019; Jones et al. 2014; Mitteldorf 2016, 2018) expressed through regulation of highly conserved pathways (Guarente and Kenyon 2000; Fontana et al. 2010) and modulation of gene expression (Kim et al. 2011; Fushan et al. 2015).

Long-lived animal models are frequently used when trying to discover the molecular bases of mammalian

longevity (Selman et al. 2009; Wu et al. 2013; Fushan et al. 2015; Ma and Gladyshev 2017; Sahm et al. 2018), and the same is true of studies comparing animal species with different longevity (Barja 1998; Perez-Campo et al. 1998; Pamplona et al. 2002; Jové et al. 2013; Naudí et al. 2013; Ma et al. 2016; Bozek et al. 2017; Mota-Martorell et al. 2019), investigations inducing genetic manipulations, and pharmacological and nutritional interventions increasing longevity (Pamplona and Barja 2006, 2011; Longo et al. 2015).

Phenotypic features associated with long-lived animal species include a lower generation of endogenous damage, highly resistant macromolecular components concerning nucleotides in DNA, proteins and lipids, and the specific transcriptomics and metabolomics profiles, among others (Pamplona and Barja 2007, 2011; Naudí et al. 2013; Ma and Gladyshev 2017; Lewis et al. 2018; Tyshkovskiy et al. 2019). Notably, several of these features seem to be supported by specific cell signalling pathways (Barja 2019), including the mechanistic target of rapamycin (mTOR) pathway.

mTOR, a member of an evolutionary conserved group of serine/threonine kinases from the PIKK (phosphatidylinositol-3 kinases (PI3K)–related kinase) family, is present as two distinct complexes: mTOR complex 1 (mTORC1) and mTOR complex 2 (mTORC2) (Valvezan and Manning 2019). mTORC1 is sensitive to rapamycin and plays a central role in the mTOR signalling network monitoring and integrating a broad diversity of extra- and intracellular signals controlling cell physiology. Thus, mTORC1 can regulate cell metabolism, growth, and proliferation and can modulate complex physiological processes such as ageing and longevity (Kapahi et al. 2010; Antikainen et al. 2017; Weichhart 2018; Papadopoli et al. 2019; Barja 2019; Valvezan and Manning 2019) through a wide range of downstream pathways such as mRNA translation, biosynthesis pathways, mitochondrial function, autophagy, endoplasmic reticulum stress, and stress responses, among others. Inhibition of the highly conserved mTOR pathway results in longevity extension in several animal models from yeast to mice (Kapahi et al. 2010; Lushchak et al. 2017; Weichhart 2018; Papadopoli et al. 2019), and mTOR activation shortens longevity, likely through downregulation of ageing and ageing-associated degenerative diseases including cancer, diabetes, and neurodegeneration (Kapahi et al. 2010; Johnson et al. 2013; Papadopoli et al. 2019).

In mammals, mTORC1 is composed of mTOR and its associated proteins Raptor (regulatory associated protein of TOR), mLst8 (mammalian lethal with SEC13 protein 8), PRAS40 (proline-rich AKT1 substrate of 40 kDa), and Deptor (DEP domain-containing mTOR-interacting protein) (Valvezan and Manning 2019). Importantly, Raptor and PRAS40 are present exclusively in mTORC1. mTOR, Raptor, and mLST8 are core components, and DEPTOR and PRAS40 are inhibitory subunits. FK506-binding protein (FKBP12) is a regulatory subunit of the rapamycin-sensitive mTORC1 activity. Extra- and intracellular signals regulating mTORC1 include growth factors, hormones, glucose, ATP, oxygen, metabolic intermediates, and amino acids (Valvezan and Manning 2019). Among amino acids, arginine, leucine, and methionine cycle metabolites play a relevant role as activators of mTORC1 through their interaction with several intracellular mediators (Valvezan and Manning 2019).

Despite the high evolutionary conservation of the mTORC1, to our knowledge, the possible existence of relevant differences in mTORC1 and its regulatory component levels across mammalian species with different longevity has never been investigated. In order to examine molecular traits associated with mammalian longevity, we used droplet digital PCR (ddPCR) and western blot methods to define the steady-state levels of gene expression and protein content of the mTORC1, and targeted metabolomics to measure the concentration of its activators. Heart tissue of eight mammalian species showing more than one order of magnitude of difference in longevity—from 3.5 years in mice to 46 years in horses—was analysed. The choice of selected subunits was the following: (i) mTOR, Raptor, and PRAS40 as exclusive components of the mTORC1; (ii) FKBP12 as regulatory subunit of the mTORC1 activity; and (iii) arginine, leucine, methionine, and its related metabolites as activators of the mTORC1 activity. Our results suggest that species-specific modulation on the mTORC1 might have contributed to extend longevity during evolution of long-lived animals.

## Methods

### Animals

Mammalian species included in this investigation study were male adult specimens with a chronological age

equivalent to the first 15–30% of their (maximum) longevity. The longevity recorded values for each species (in years) were the following: mouse (*Mus musculus*), 3.5; rat (*Rattus norvegicus*), 4.5; gerbil (*Meriones unguiculatus*), 6.3; guinea pig (*Cavia porcellus*), 8; rabbit (*Oryctolagus cuniculus*), 13; pig (*Sus scrofa*), 27; cow (*Bos taurus*), 30; and horse (*Equus caballus*), 46. Rodents and rabbits were obtained from rodent husbandries and sacrificed by decapitation, whereas sheep, pigs, cow, and horses were obtained from abattoirs. The animal care protocols were approved by the Animal Experimentation Ethics committee of the University of Lleida. Heart ventricles from 5 to 7 animals were removed and immediately frozen in liquid nitrogen and transferred to  $-80^{\circ}\text{C}$  until analyses.

#### Sample homogenisation and quantification

Heart tissue ( $\approx 50$  mg of whole tissue) was homogenized in a buffer containing 180 mM KCl, 5 mM MOPS, 2 mM EDTA, and 1 mM DTPAC adjusted to pH = 7.4. Prior to homogenisation, 1  $\mu\text{M}$  BHT and a mix of proteases inhibitors (GE80-6501-23, Sigma, Madrid, Spain) and phosphatase inhibitors (1 mM  $\text{Na}_3\text{VO}_4$ , 1 M NaF) were added. After a brief centrifugation (1000 rpm for 3 min at  $4^{\circ}\text{C}$ ), supernatants' protein concentration was measured using the Bradford method (500-0006, Bio-Rad Laboratories, Barcelona, Spain).

#### Protein content determination

The amount of mTORC1 core elements mTOR and its phosphorylation mTOR<sup>Ser2448</sup>, PRAS40 and its phosphorylation PRAS40<sup>Thr246</sup>, and Raptor, as well as its negative regulator FKBP12, was estimated using western blot analyses as previously described by Gomez et al. 2015.

Briefly, heart homogenates were mixed with a buffer containing 62.5 mM Tris-HCl pH 6.8, 2% SDS, 10% glycerol, 20%  $\beta$ -mercaptoethanol, and 0.02% bromophenol blue, and heated for 3 min at  $95^{\circ}\text{C}$ . Then, proteins were subjected to one-dimensional electrophoresis on SDS and transferred to PVDF membranes. Membranes were maintained in blocking solution containing Tris 2 M, NaCl 2.5 M, 5% BSA, and 0.01% Tween for 1 h at room temperature. Immunodetection was performed using antibodies against mTOR (2972, Cell signalling, Barcelona, Spain), mTOR<sup>Ser2448</sup> (2971, Cell Signalling, Barcelona, Spain), PRAS40 (ab151718,

Abcam, Cambridge, UK), PRAS40<sup>Thr246</sup> (ab134084, Abcam, Cambridge, UK), Raptor (ab189158, Abcam, Cambridge, UK), and FKBP12 (ab2981, Abcam, Cambridge, UK). Secondary antibodies were anti-mouse (GENA931, Sigma, Madrid, Spain) and anti-rabbit (31460, Thermo Fisher, Barcelona, Spain). Bands were visualized using an enhanced chemiluminescence HRP substrate (Millipore, MA, USA). Signal quantification and recording were performed with ChemiDoc equipment (Bio-Rad Laboratories, Barcelona, Spain). Protein amount was calculated from the ratio of their densitometry values referred to the densitometry values of their own total protein content (for phosphorylated proteins, mTOR<sup>Ser2448</sup> and PRAS40<sup>Thr246</sup>) and its respective Coomassie staining (1610436, Bio-Rad Laboratories, Barcelona, Spain) (Supplementary Fig. 3). Protein densitometry values are reported in the dataset.

#### Primer design

Gene cDNA sequences coding for the mTORC1 elements mTOR (*mtor*), PRAS40 (*akt1s1*), and Raptor (*rptor*), as well as its negative regulator FKBP12 (*fkbp1a*), were obtained from Ensembl (<http://www.ensembl.org>). Due to gene cDNA sequence limitations for gerbil, that species was not included in the gene expression analyses. Degenerate primers were designed to amplify conserved regions among mammalian sequences using the software PriFi (Fredslund et al. 2005) and are listed in Supplementary Table 2. Primers were purchased from Isogen (Life Sciences, Utrecht, Netherlands).

#### Gene expression: droplet digital PCR

Prior to DNA amplification, RNA from 15 mg whole heart tissue was extracted using RNeasy Fibrous Tissue Mini Kit (Qiagen, Hilden, Germany) and reverse-transcribed to cDNA using the High-Capacity cDNA Reverse Transcription Kit (Applied Biosystems, CA, USA).

For DNA amplification, reaction mixture contained  $1\times$  of EvaGreen ddPCR Supermix, 200 nM primers, and 0.01–16 ng of template cDNA. For droplet generation, 20  $\mu\text{L}$  of reaction mixture and 70  $\mu\text{L}$  of Droplet Generation Oil for EvaGreen were loaded in the droplet generation cartridge, which was placed into the droplet generator. From each PCR reaction mixture, 20  $\mu\text{L}$  were transferred to a 96-well PCR plate, which was sealed

with a foil heat using PX1 PCR plate sealer. Amplification was performed in a C1000 Touch Thermal Cycler following an initial DNA polymerase activation (95 °C, 5 min), and 40 cycles consisting of a DNA denaturation (95 °C, 30 s), primer annealing (58 °C, 1 min), and extension (60 °C, 1 min). A final dye-stabilization step was included (4 °C 5 min and 90 °C 5 min). Droplets were read with a QX200 Droplet Reader and analysed using the QuantaSoft software (Bio-Rad). The results from more than 12,000 droplets were accepted and normalised to an appropriate housekeeping gene (*ndufa9*) as suggested by Miwa et al. 2014. Values are reported as cDNA gene units per cDNA housekeeping units. Since no amplification was obtained for PRAS40 (*akt1s1*), it was removed from the analyses. Gene cDNA units are reported in the dataset. All equipment and reagents were purchased from Bio-Rad (Bio-Rad Laboratories, Barcelona, Spain).

## Targeted metabolomics

### Sample processing

Tissue metabolite extraction was performed based on the methodology previously described (method 1, Cabré et al. 2016). Briefly, 10 µL of sample homogenates was added to 30 µL of cold methanol containing 1 µg/mL of Phe-<sup>13</sup>C as internal standard and 1 µM BHT as antioxidant. Then, samples were incubated at room temperature for 15 min and centrifuged at 12,000g for 3 min. Finally, the supernatant was filtrated through a 0.22-µm organic diameter filter (CLS8169, Sigma, Madrid, Spain) and 200 µL was transferred to Agilent (Barcelona, Spain) vials with glass inserts for further analysis.

Sulphur-containing metabolites were extracted on the bases of the methodology previously described (method 2, Liu et al. 2017). Briefly, 2 µL of 5% DTT was added to 10 µL of sample homogenates. The resulting solution was vortexed for 1 min and allowed to stand at room temperature for 10 min. For protein precipitation, 40 µL of 0.1% formic acid plus 0.05% trifluoroacetic acid in acetonitrile containing 1 µg/mL of Phe-<sup>13</sup>C as internal standard was added to the sample, and the solution was vortexed for 2 min. Then, samples were incubated at room temperature for 15 min and centrifuged at 12000g for 3 min. Finally, the supernatant was filtrated through a 0.22-µm organic diameter filter (CLS8169, Sigma, Madrid, Spain) and 200 µL was transferred to Agilent (Barcelona, Spain) vials with glass inserts for further analysis.

### Analysis conditions

The individual conditions for the detection and quantification of heart metabolites are listed in Supplementary Table 3. For non-sulphur-containing metabolites, 2 µL of extracted sample was injected based on the method described (method 1, Cabré et al. 2016). Chromatographic separation was achieved on a reversed-phase column (Zorbax SB-Aq 1.8 µm 2.1 × 50 mm, Agilent Technologies, Barcelona, Spain) equipped with a pre-column (Zorba-SB-C8 Rapid Resolution Cartridge 2.1 × 30 mm 3.5 µm, Agilent Technologies, Barcelona, Spain) with a column temperature of 60 °C. The flow rate was 0.6 mL/min during 19 min. Solvent A was composed of water containing 0.2% acetic acid and solvent B was composed of methanol 0.2% acetic acid. The gradient started at 2% B and increased to 98% B in 13 min and held at 98% B for 6 min. Post-time was established in 5 min. Electrospray ionization was performed in both positive and negative ion mode (depending on the target metabolite) using N<sub>2</sub> at a pressure of 50 psi for the nebuliser with a flow of 12 L/min and a temperature of 325 °C, respectively.

For sulphur-containing metabolites, 10 µL of extracted sample was injected based on the method described (method 2, Liu et al. 2017). Chromatographic separation was achieved on a reversed-phase Supelcosil LC-CN column (Supelco of 4.6 × 250 mm and 5 µL particle size, Sigma, Madrid, Spain) with a column temperature of 30 °C. The flow rate was 0.5 mL/min during 10 min at 10% B. Solvent A was composed of water containing 0.1% formic acid and solvent B was composed of acetonitrile 0.1% formic acid. Electrospray ionization was performed in both positive and negative ion mode (depending on the target metabolite) using N<sub>2</sub> at a pressure of 50 psi for the nebuliser with a flow of 12 L/min and a temperature of 325 °C, respectively.

Data was collected using the MassHunter data analysis software (Agilent Technologies, CA, USA). Peak determination and peak area integration were carried out with MassHunter quantitative analyses (Agilent Technologies, CA, USA).

### Metabolite quantification

Metabolite quantification was performed by constructing standard curves for each metabolite. Expected tissue concentration for each metabolite was based on the Human Metabolome Database (HMDB, <http://www>).

hmdb.ca). Standard curves were constructed by plotting the peak area ratio against the final metabolite concentration. Metabolite concentration per amount of tissue is reported in the dataset.

### Equipment

The analysis was performed through liquid chromatography coupled to a hybrid mass spectrometer with electrospray ionization and a triple quadrupole mass spectrometer. The liquid chromatography system was an ultra-performance liquid chromatography model 1290 coupled to ESI-TQ MQ/MS model 6420 both from Agilent Technologies (Barcelona, Spain).

### Statistics

Multivariate statistics was performed using the Metaboanalyst software (Chong et al. 2019). Pearson correlation and Pearson partial correlation were performed using RStudio (v1.1.453). Linear models and phylogenetic generalised least squares regression (PGLS) were constructed using RStudio (v1.1.453). The phylogenetic tree was constructed using taxon names according to Kumar et al. 2017. Functions used were included in the package *caper*. Data was log-transformed and mean-centred prior statistical analyses in order to accomplish the assumptions of linearity.

## Results

### Multivariate statistics reveals a species-specific mTORC1 profile

In order to determine whether heart mTORC1 gene expression and protein content, and the concentration of its regulators differed among mammals, multivariate statistics were applied using the levels of gene expression of *mtor*, *rptor*, and *fbp1a*, protein content of mTOR and its phosphorylation (measured as mTOR<sup>Ser2448</sup>/mTOR ratio), PRAS40 and its phosphorylation (measured as PRAS40<sup>Thr246</sup>/PRAS40) and FKBP12, and concentration of the amino acids leucine, arginine, methionine, and the methionine cycle metabolites SAH, SAM, and homocysteine. Non-supervised principal component analysis (PCA) revealed the existence of a species-specific protein and gene profile of the mTORC1 (Fig. 1(a)), capable to explain up to 45.1% of

sample variability. A hierarchical clustering of the samples represented by a heat map revealed specific mTORC1 patterns for rodents (mouse, rat, and guinea pig) (Fig. 1(b)). Furthermore, this global pattern found in rodents was different from that found in non-rodents (rabbit, pig, cow, and horse) (Fig. 1(c)). These results were confirmed by performing a supervised analysis, such as partial least squares discriminant analysis (PLS-DA) (Fig. 1(d)). However, cross-validation values of PLS-DA model showed that heart gene expression and protein amount of mTORC1, and the content of its regulators, are a limited model to define the animal species scoring a  $R^2 = 0.6$  and  $Q^2 = 0.4$ , obtaining a maximum accuracy of 0.5 using 2 components (Fig. 1(e)). Permutation tests (2000 repeats) yielded a low  $p = 0.006$ , indicating that none of the distributions formed by the permuted data was better than the observed statistic based on the original data (Fig. 1(f)). The discriminating power between groups of the different measured features was ranked by applying a variable importance projection (VIP) score (Fig. 1(g)). After selecting those features with VIP score  $> 1.5$  as significant, the *mtor* gene expression and FKBP12 protein content were found to be the top-ranked features.

The species-specific mTORC1 profile is associated with species longevity

The gene expression and protein content of mTORC1 were also correlated with species longevity (Fig. 2). Specifically, long-lived animals have increased *mtor* expression, but decreased *Raptor* (Fig. 2(a)). Long-lived animals also had less protein content of mTOR and Raptor but higher PRAS40 (Fig. 2(b)). Furthermore, gene expression and protein content of Raptor were positively correlated (Supplementary Fig. 1). Regarding protein phosphorylation, increased mTOR<sup>Ser2448</sup>/mTOR and decreased PRAS40<sup>Thr246</sup>/PRAS40 were found in long-lived animals (Fig. 2(c)). Interestingly, the protein content of mTOR and PRAS40 is inversely correlated with their degree of phosphorylation (Supplementary Fig. 1).

The mTORC1 profile is associated with its regulators and methionine metabolites

Due to the relevance of regulatory factors such as FKBP12 and specific metabolites like arginine, leucine, and methionine cycle components in determining

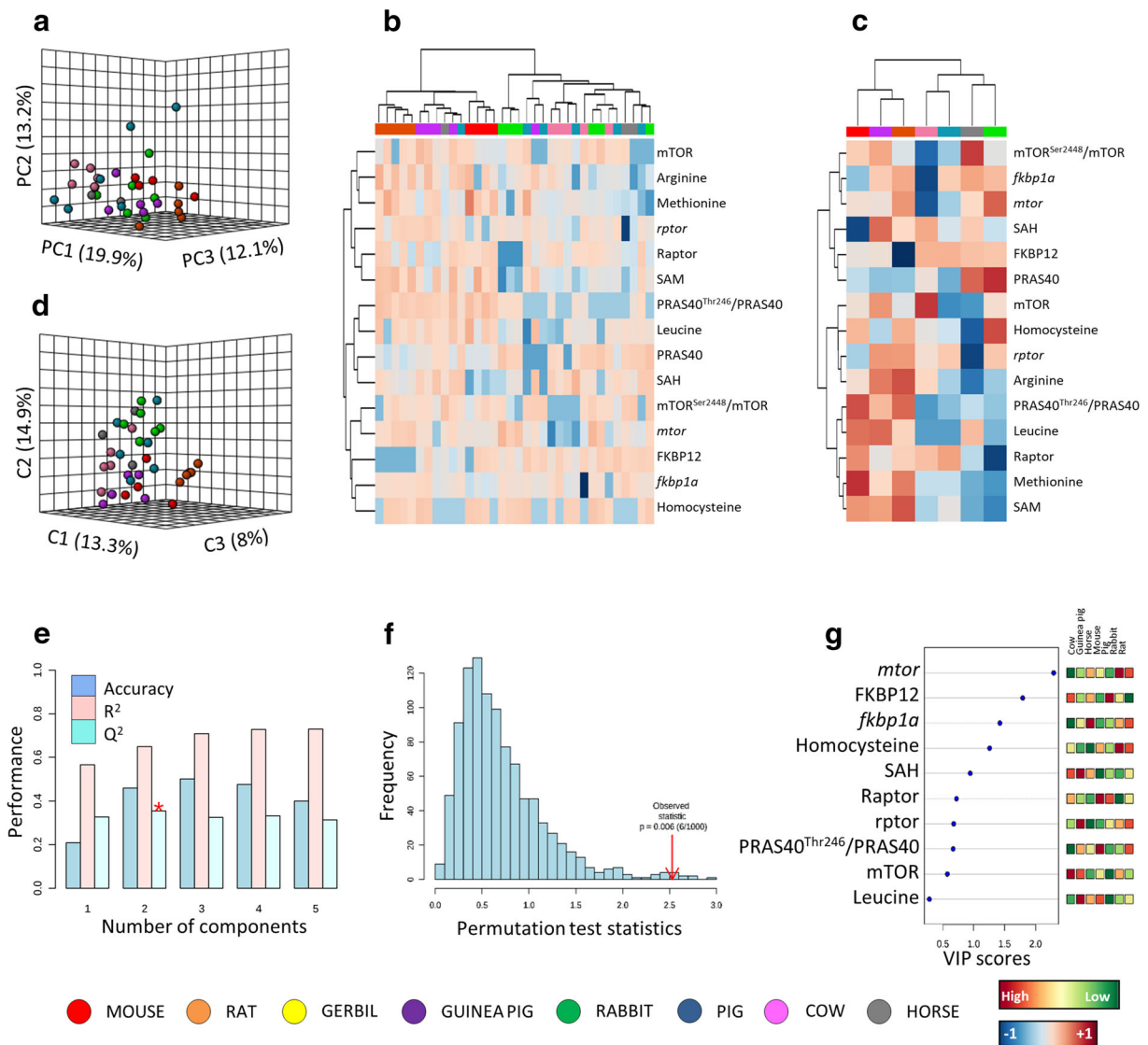


**Fig. 1** Multivariate statistics reveals a species-specific gene expression and protein content and phosphorylation of mTORC1 subunits, and metabolite concentration of its regulators. (a) Principal component analyses (PCA) representation of gene expression and protein content and phosphorylation of mTORC1, and metabolite concentration ( $\mu\text{M}/\text{mg}$  of heart tissue) of its regulators. X, principal component 1 (PC1); Y, principal component 2 (PC2); Z, principal component 3 (PC3). (b) Hierarchical clustering of individual animal samples according to gene expression and protein content and phosphorylation of mTORC1, and metabolite concentration ( $\mu\text{M}/\text{mg}$  of heart tissue) of its regulators. (c) Hierarchical clustering of animal species according to average sample

values of gene expression and protein content and phosphorylation of mTORC1, and metabolite concentration ( $\mu\text{M}/\text{mg}$  of heart tissue) of its regulators. (d) Partial least squares discriminant analysis (PLS-DA) representation of gene expression and protein content and phosphorylation of mTORC1, and metabolite concentration ( $\mu\text{M}/\text{mg}$  of heart tissue) of its regulators. X, component 1 (C1); Y, component 2 (C2); Z, component 3 (C3). (e) Cross-validation (CV) analyses (10-fold CV method) of the PLS-DA model. (f) Permutation test (1000 repeats) using separation distance. (g) Variable importance projection (VIP) scores indicating the elements which contribute most to define the first component of a PLS-DA

mTORC1 activity, we have evaluated their relationship with species longevity and mTORC1 core components (Fig. 3). Thus, two well-known positive activators of mTOR, arginine, and methionine (Fig. 4(a)), as well as

two methionine-related metabolites, such as SAM and homocysteine (Fig. 4(b)), were found to be negatively correlated with mammalian longevity. Gene expression of *fkbp1a* and protein content of FKBP12 were also

negatively correlated with longevity (Fig. 4(c)). Therefore, the greater the longevity of a mammalian species, the lower is the tissue concentration of the mTORC1 regulatory metabolites. In addition, methionine metabolites were associated with mTOR, PRAS40, and Raptor (Fig. 3). Accordingly, methionine and SAM were positively associated to Raptor and PRAS40<sup>Thr246</sup>/PRAS40, but negatively related to PRAS40; SAM was also negatively correlated with mTOR<sup>Ser2448</sup>/mTOR, whereas homocysteine was positively correlated with PRAS40<sup>Thr246</sup>/PRAS40 (Fig. 5). Arginine was positively correlated with PRAS40<sup>Thr246</sup>/PRAS40 and FKBP12, but negatively with PRAS40 (Fig. 6). Finally, the regulatory factor FKBP12 showed a positive correlation with *rptor* and Raptor, and a negative correlation with phosphorylated mTOR (Fig. 6).

#### mTORC1 longevity changes are independent of phylogenetic relationships

Animal species are evolutionary related, raising the possibility that data from closely related species might not be statistically independent from one another. Therefore, to correct for phylogeny, we performed a PGLs following the phylogenetic tree constructed in Fig. 7(a). First of all, we have measured the amount of phylogenetic signal of each trait (Pagel's  $\lambda$ ). Basically, it indicates the degree up to which a specific trait is influenced by phylogeny, indicating whether the changes in those traits across different species might be due ( $\lambda = 1$ ) or not ( $\lambda = 0$ ) to phylogenetic relationships. After correcting for phylogeny, the expression of *mtor* ( $p = 0.008$ ,  $r = -0.20$ ), *rptor* ( $p = 0.008$ ,  $r = 0.05$ ) and *fkbp1a* ( $p = 0.019$ ,  $r = -0.16$ ), mTOR<sup>Ser2448</sup>/mTOR ( $p = 0.023$ ,  $r = -0.94$ ), PRAS40<sup>Thr246</sup>/PRAS40 ( $p = 0.023$ ,  $r = -0.66$ ), methionine ( $p = 0.011$ ,  $r = 0.17$ ), and SAM ( $p = 0.049$ ,  $r = 0.11$ ) continued to be correlated with mammalian longevity (Fig. 7(b), Supplementary Fig. 2, Supplementary Table 1).

## Discussion

### Longevity-associated mTORC1 profile

We have found that animal species have a unique species-specific mTORC1 profile, which is associated with animal longevity. Furthermore, our results revealed that mTORC1 accounts for 60% of inter-species

variation in longevity, mTORC1 gene expression, and protein phosphorylation being the strongest longevity predictors. In agreement with this, previous studies have already described a unique gene expression profile (Fushan et al. 2015; Caron et al. 2015; Ma et al. 2016; Muntané et al. 2018), metabolome (Ma et al. 2015), and lipidome (Jové et al. 2013; Mota-Martorell et al. 2019) in long-lived species. Since mTORC1 is a master regulator of cellular metabolism including mRNA translation and lipid synthesis (Caron et al. 2015), those findings support the existence of important genetic adaptations in nutrient-sensing metabolic pathways, including those up- or downstream of mTOR, in the evolution of longevity (Singh et al. 2019).

### Decreased mTORC1 content and activity to achieve a high longevity phenotype

Decreasing mTORC1 content and activity is associated with superior species longevity phenotypes. Long-lived animal species have decreased *rptor* but increased *mtor*. Accordingly, it has been reported that nonagenarians' blood has decreased mRNA content of *akt1s1* (PRAS40) and *rptor* (Raptor) when compared with middle-aged controls (Passtoors et al. 2013). Moreover, the offspring of those long-lived individuals also has decreased *rptor* gene expression, which emerges as a potential biomarker of familial longevity (Passtoors et al. 2013). In the present investigation, protein content of mTOR and Raptor was also lower in long-lived animals, supporting a role for Raptor in longevity.

mTORC1 is regulated by opposite phosphorylation patterns in mTOR and PRAS40. Phosphorylation of mTOR at serine 2448 has inhibitory effects in skeletal muscle (Figueiredo et al. 2017). Nutrient availability promotes mTOR activation that, in turn, activates p70S6K which re-phosphorylates mTOR (at Ser<sup>2448</sup>) inhibiting its activity. The existence of this negative feedback loop could explain why some studies found that starvation increases Ser<sup>2448</sup> (Chiang and Abraham 2005). Proline-rich AKT substrate 40 kDa (PRAS40) is a component and negative regulator of the mTOR complex (Sancak et al. 2007). However, PRAS40 phosphorylation at Thr<sup>246</sup> via Akt results on its dissociation from mTORC1 activating it (Nascimento et al. 2010). In agreement with this, we have found increased mTOR<sup>Ser2448</sup>/mTOR and PRAS40, but decreased PRAS40<sup>Thr246</sup>/PRAS40 in long-lived animals, all these three differences tending to inhibit mTORC1,

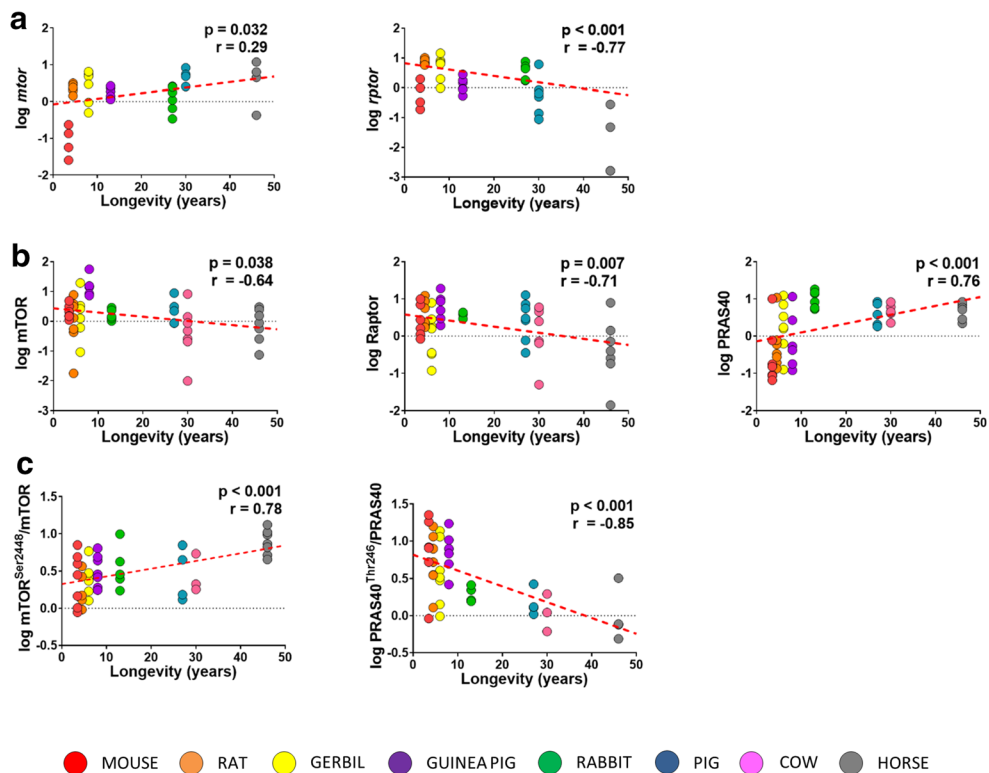


**Fig. 2** mTORC1 gene expression (a), protein content (b), and phosphorylation (c) are linearly correlated with mammalian longevity. Pearson correlations were performed between gene expression, protein content or phosphorylation, and longevity. Linear regression was applied when significant relationships were found.  $R^2(mtor) = 0.1$ ;  $R^2(rptor) = 0.40$ ;  $R^2(mTOR) < 0.1$ ;  $R^2(Raptor) =$

$0.14$ ;  $R^2(PRAS40) = 0.22$ ;  $R^2(mTOR^{Ser2448}/mTOR) = 0.27$ ;  $R^2(PRAS40^{Thr246}/PRAS40) = 0.40$ . Minimum significance level was set at  $p < 0.05$ . Gene expression, and protein content and phosphorylation were log-transformed to accomplish the assumptions of normality

suggesting that this inhibition is one among the various different signals to the nucleus that modulate gene expression of specific longevity-related genes. This, in turn, modulates protein synthesis of multiple ageing effectors in the cytosolic or extracellular compartments, to finally cooperate together in the production of a high longevity phenotype (Barja 2019). Previous studies had already reported inhibitory changes at mTORC1 activators in whales with an estimated longevity of 200 years (Ma and Gladyshev 2017). Genetic mutations downregulating mTOR downstream signalling (Wu et al. 2013) or its downstream effector S6K1 (Selman et al. 2009) increase lifespan in mice, similarly to its pharmacological inhibition by rapamycin (Singh et al. 2019). Furthermore, the lower phosphorylation of PRAS40-Thr<sup>246</sup> in long-lived animal species suggests a lower activation of AKT (the major kinase promoting PRAS40-Thr<sup>246</sup> phosphorylation is Akt (Nascimento et al. 2010)) probably associated with a downregulation of the insulin

signalling pathway which is a conserved regulatory system for ageing and longevity (Kenyon 2010). Further studies are, however, needed to develop a more detailed view.

Achievement of superior longevity is not exclusively due to changes on mTORC1 itself, but also on its activity regulators. Although it might sound controversial, decreased gene expression and protein content of the inhibitor FKBP12 was found in long-lived animals. However, since mTORC1 total content is decreased, less inhibitor is needed, allowing to save the energy that otherwise will be used to synthesize those protein. Besides, recent studies have revealed that FKBP12 is associated with neurotoxicity (Caraveo et al. 2017), and its disruption enhances mTOR-Raptor interactions and memory (Hoeffler et al. 2008). Therefore, our results suggest that maintenance of proper mTORC1 stability by decreasing FKBP12 might be a molecular trait of mammalian longevity.

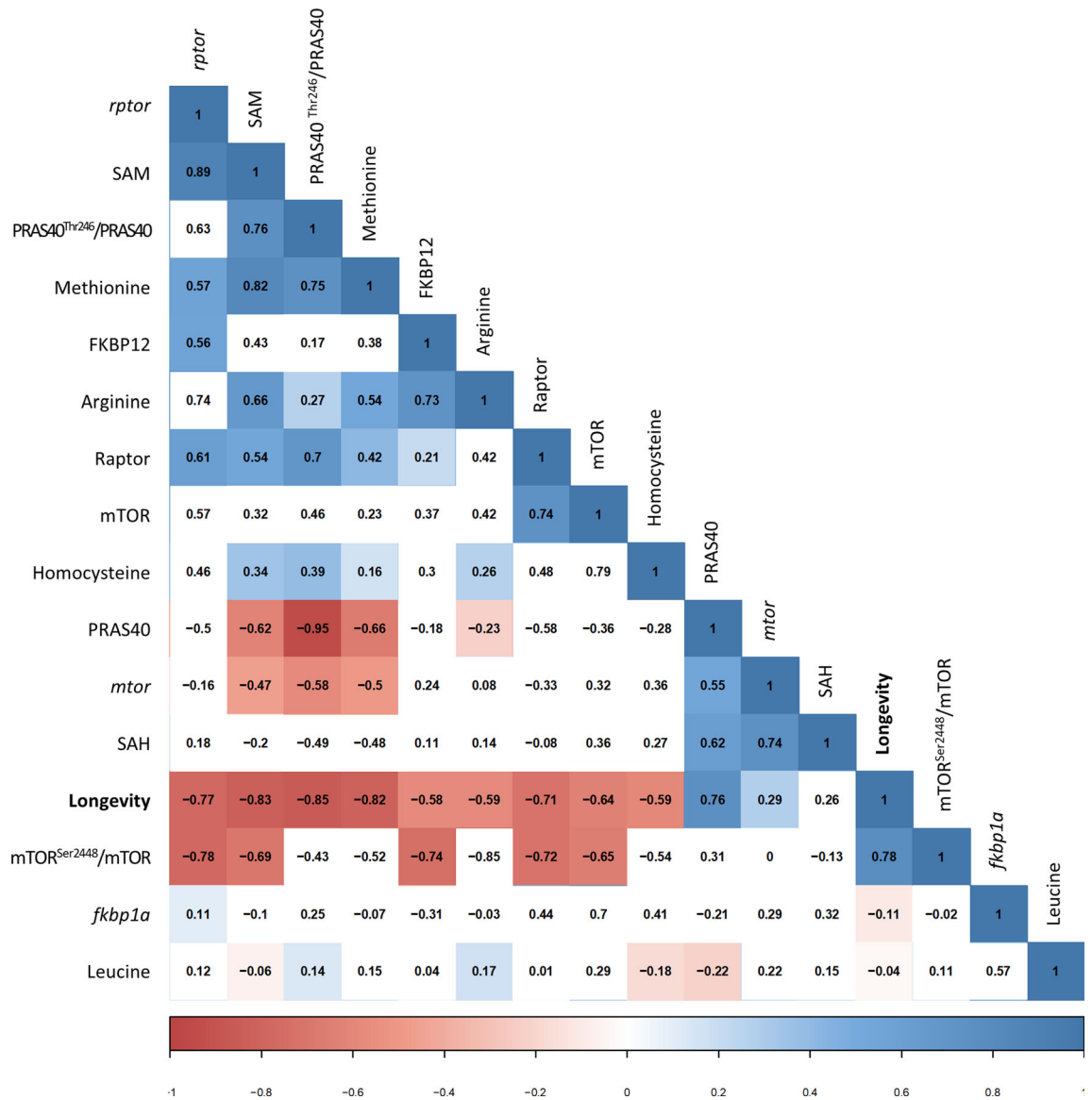


**Fig. 3** Gene expression, protein content, and phosphorylation of mTORC1 subunits are correlated with metabolite concentration of its regulators. Pearson *r* value for pairwise comparisons is reported. Non-significant correlations are left in blank. Minimum

signification level was set at  $p < 0.05$ . Gene expression, protein content and phosphorylation, and metabolite concentration ( $\mu\text{M}/\text{mg}$  of heart tissue) were log-transformed to accomplish the assumptions of normality

Decreased concentration of mTORC1 activators, such as arginine and methionine-related metabolites, might enhance its downregulation. Accordingly, arginine content in primate fibroblasts is negatively correlated with longevity (Ma et al. 2016), and naked mole rats have lower levels of plasma methionine than mice (Lewis et al. 2018), and increased methionine, SAM, and homocysteine have been observed in ageing mice liver (Jeon et al. 2018).

### mTORC1 and methionine metabolism: the longevity connexion

mTORC1 is often described as a master regulator of cellular metabolism, due to its capacity to modulate anabolic and catabolic processes such as protein turnover. It has been proposed that mTORC1 inhibition during dietary restriction promotes autophagy, which clears old and dysfunctional organelles, promoting

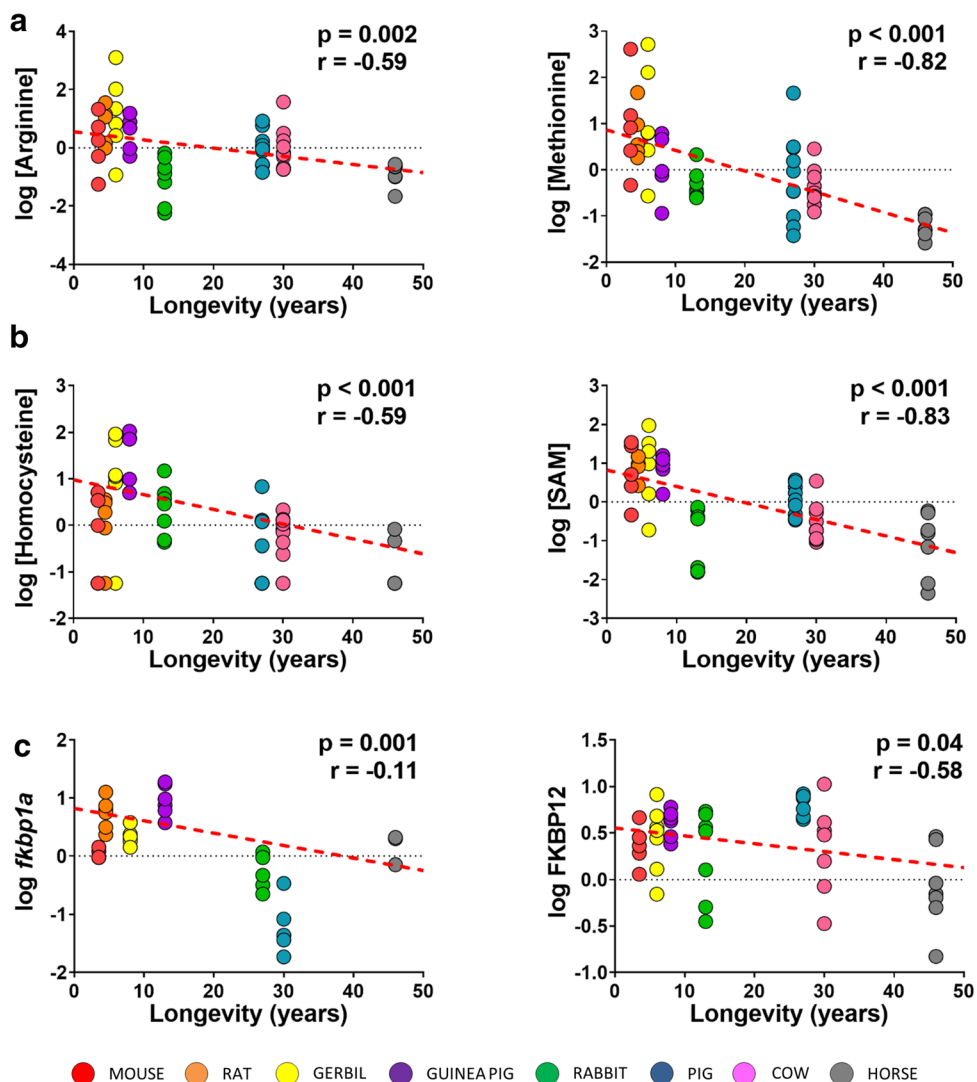


**Fig. 4** Regulatory factors of mTORC1 are correlated with mammalian longevity. (a) Correlation between amino acids (arginine and methionine) and animal ML. (b) Correlation between methionine cycle metabolites (SAM and homocysteine) and species longevity. (c) Correlation between FKBP12 gene expression and protein content and longevity. Pearson correlation was performed between longevity and gene expression, protein content and phosphorylation, and metabolite concentration ( $\mu\text{M}/\text{mg}$  of heart tissue).

lifespan extension (Simonsen et al. 2008). Supporting this idea, it was found that phenotypic expression of the methionine restriction life extension effect requires autophagy (Ruckenstuhl et al. 2014; Bárcena et al. 2019). Furthermore, a study in worms demonstrated that SAMTOR, a regulator of mTOR, detects methionine availability via SAM and is also involved in longevity extension during dietary restriction (Gu et al. 2017). Overall, these results support that autophagy induction

Pearson  $r$  values are reported in Fig. 3. Linear regression was applied when significant relationships were found.  $R^2$ (methionine) = 0.42;  $R^2$ (arginine) = 0.16;  $R^2$ (SAM) = 0.38;  $R^2$ (homocysteine) = 0.24;  $R^2$ (*fkbp1a*) = 0.33;  $R^2$ (FKBP12) < 0.1. Minimum significance level was set at  $p < 0.05$ . Gene expression, protein content, and metabolite concentration were log-transformed to accomplish the assumptions of normality

via mTORC1 downregulation or inhibition might be among the various key mechanisms promoting a long lifespan.

In our model, we have been able to establish a correlation between the mTORC1-longevity associated changes and the methionine metabolism. Specifically, we have found that methionine, homocysteine, and arginine might influence PRAS40 phosphorylation, whereas SAM could influence mTOR phosphorylation.

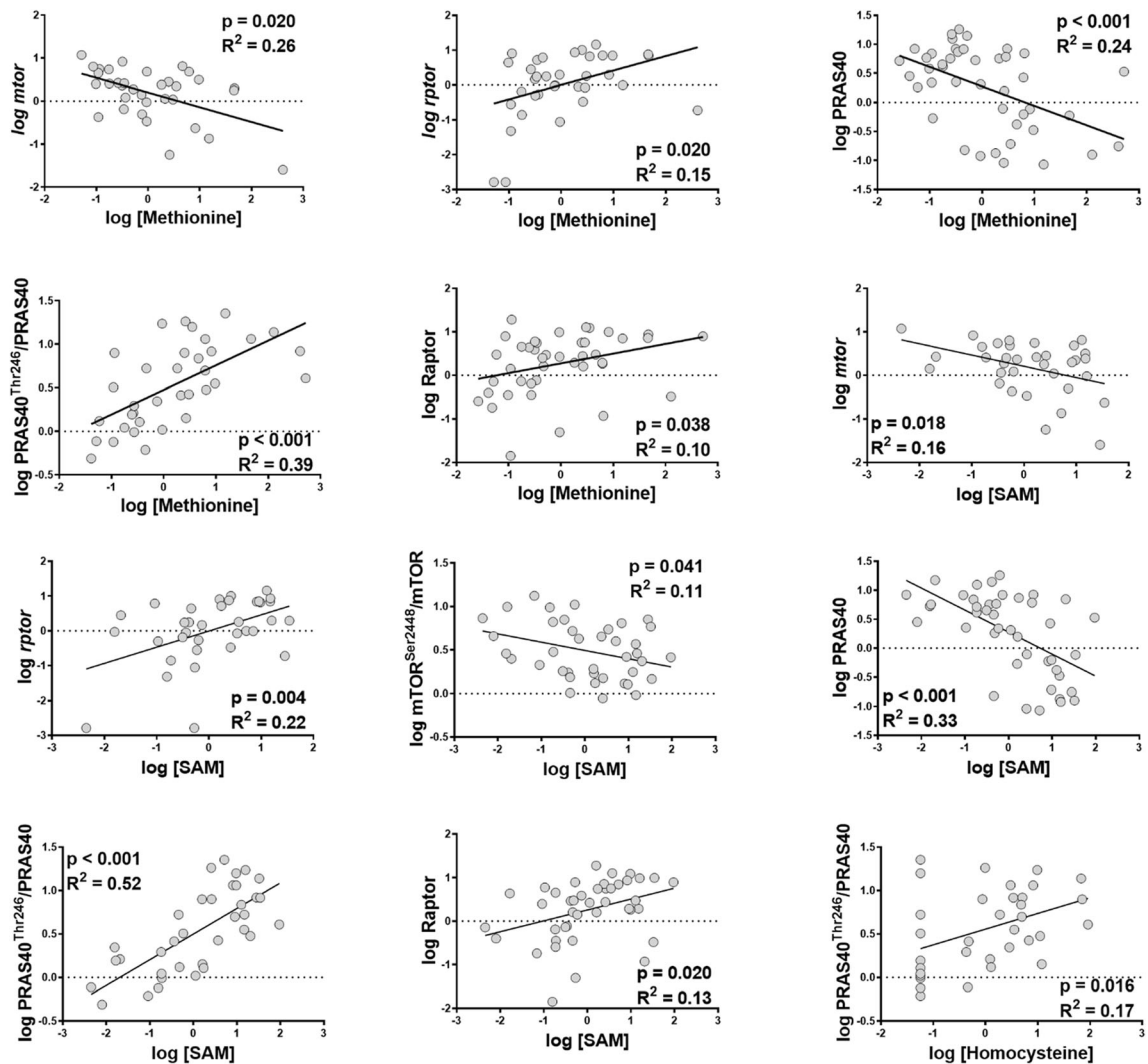


**Fig. 5** mTORC1 and methionine-related metabolites are correlated in heart tissue from mammalian species. Pearson correlation was performed among gene expression, protein content or phosphorylation, and metabolite concentration ( $\mu\text{M}/\text{mg}$  of heart tissue). Pearson  $r$  values are reported in Fig. 3. Linear regression (LR)

Furthermore, methionine and SAM levels change Raptor, supporting the idea that it might be another key factor modulating animal longevity. However, more studies concerning mTORC1 modulation in animal longevity need to be done to confirm these new insights (Fig. 8). mTORC1 activity has also been related to increased mitochondrial activity (Schieke et al. 2006; Cunningham et al. 2007), as well as increased de novo lipid biosynthesis and protein synthesis (Düvel et al. 2010), that might favour the long-lived phenotype.

model was performed when significant relationships were found. Minimum significance level was set at  $p < 0.05$ . Gene expression, protein content and phosphorylation, and metabolite concentration were log-transformed to accomplish the assumptions of normality

### Assessing inter-species issues

Comparative studies across species with different lifespan are a powerful source of information helping to identify mechanisms linked to extended longevity and to discard those not related to it (Ma et al. 2015, 2016; Bozek et al. 2017). However, those kinds of studies raise several problems that need to be addressed. First, evolutionary relationships do not allow to assume data independence (Cooper et al. 2016). Therefore, we

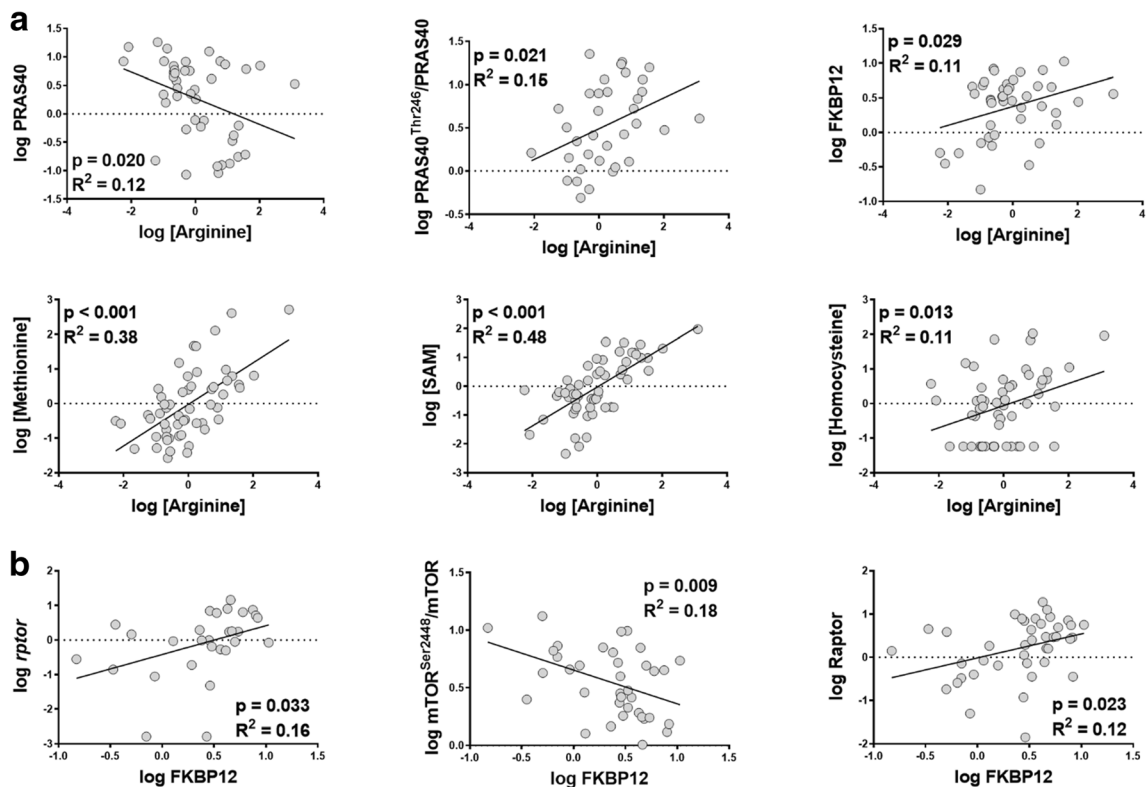


**Fig. 6** mTORC1 and its regulators arginine and FKBP12 are correlated in heart tissue of mammals. Pearson correlation was performed among gene expression, protein content and phosphorylation, and metabolite concentration. Pearson  $r$  values are reported in Fig. 3. Linear regression (LR) model was performed when

significant relationships were found. Minimum significance level was set at  $p < 0.05$ . Gene expression, protein content and phosphorylation, and metabolite concentration were log-transformed to accomplish the assumptions of normality

cannot know, in principle, if a specific trait truly correlates with longevity differences, or alternatively, whether such correlation could be due to the existence of phylogenetic similarity among the species selected. To overcome this limitation, we have carried out statistical analyses accounting for these phylogenetic relationships. In this way, we have found that phylogeny has greater influence on protein content and activity compared with gene expression, suggesting that gene expression is relevantly involved in endogenously generating the high longevity of long-lived animals. The second problem that needs to be assessed is technical, due to the presence of SNPs inducing amino acid variations. Although the mTOR pathway is highly conserved across living organisms (Fontana et al. 2010), small variations in protein amino acid sequence across species could decrease antibody recognition. To overcome these methodological

issues, we used degenerated primers capable to recognise sequences with SNPs. Furthermore, sequencing of PCR products allowed us to confirm primer specificity and gene detection.

## Conclusions

Our results, taken together, support a role for mTORC1 in the evolution of mammalian longevity. We provide new insights into the influence of gene expression, total protein content, and modulation of basal levels of mTORC1 activation on species longevity. We suggest that maintaining mTORC1 on a lowered and inhibited state during adult life, after development, growing, and maturation, is one among the main signals stimulating the cell nucleus to produce a long-lived phenotype. This is endogenously generated by varying the expression of hundreds of target genes, which changes the level of

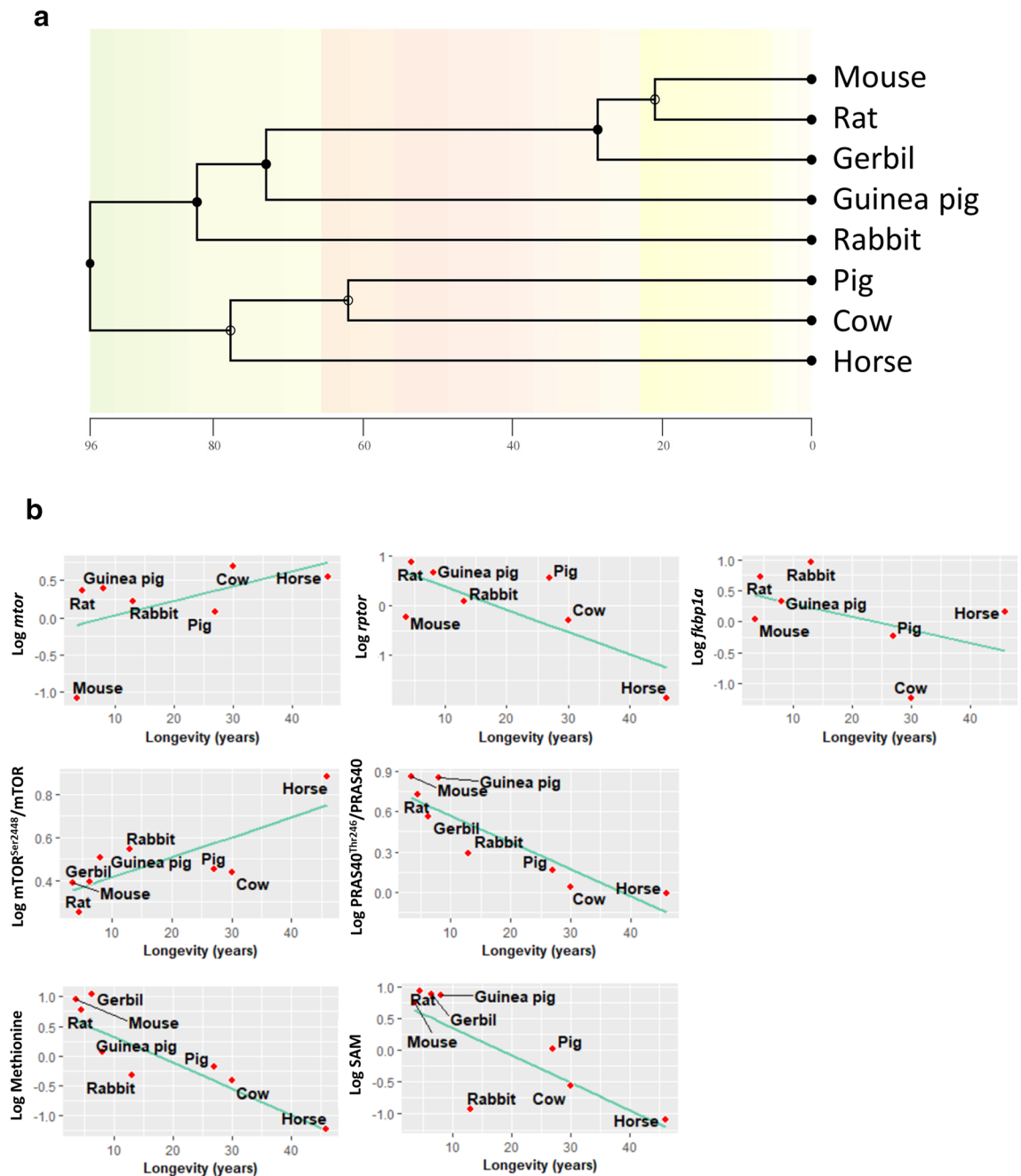


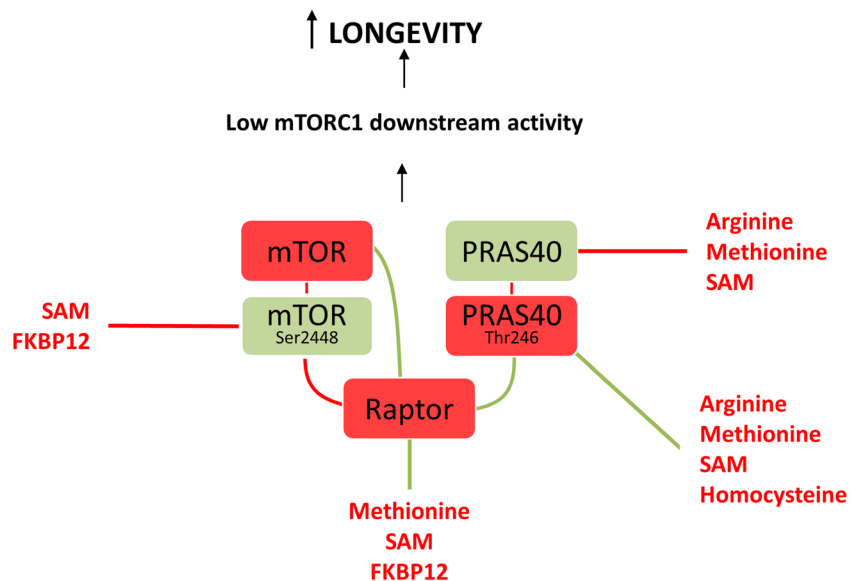
**Fig. 7** mTORC1 is correlated with animal longevity after correcting for phylogenetic relationships. (a) Phylogenetic tree with a timescale of million years ago. (b) mTORC1 subunits and regulators that are correlated with animal longevity after

performing a phylogenetic generalised least squares regression. Metabolite concentration, gene expression, and protein content were log-transformed to accomplish the assumptions of normality

activity of the multiple ageing effectors like mitochondrial ROS production, membrane fatty acid unsaturation, apoptosis, autophagy, telomere shortening, proteostasis, or inflammaging (Barja 2008, 2019).

Thereby, the mechanisms or drugs that regulate mTOR activity might prompt new insights and potential applications to humans like rapamycin, aimed to slow down the rate of human ageing.

**Fig. 8** Longevity model of the mTORC1 modulation. Coloured boxes are used to indicate increased (green boxes) or decreased (red boxes) mTORC1 elements in long-lived animals. Coloured text is used to indicate increased (green text) or decreased (red text) mTORC1 regulatory factors in long-lived animals. Coloured lines are used to indicate positive (green lines) or negative (red lines) correlations between mTORC1 and its regulatory factors, as reported in Figs. 3, 5, and 6, or among mTORC1 elements, as reported in Fig. 3 and Supplementary Fig. 1



**Acknowledgments** MJ is a ‘Serra Hunter’ Fellow. NMM received a predoctoral fellowship from the Generalitat of Catalonia (AGAUR, ref 2018FI\_B2\_00104). RB received a predoctoral fellowship from the ‘Impuls Program’ funded by the University of Lleida and Banco Santander (UdL, ref 0864/2016). We thank Salvador Batolome, from the Laboratory of Luminescence and Biomolecular Spectroscopy (Autonomous University of Barcelona, Barcelona, Catalonia, Spain), for ddPCR technical support.

**Author contributions** GB and RP designed the study. NMM, MJ, IP, RB, IS, AN, and EG performed experimental work. NMM and RP analysed the data. RP supervised the design and data interpretation. The manuscript was written by NMM, GB, and RP and edited by RP. All authors discussed the results and commented on the manuscript.

**Funding information** This work was supported by the Spanish Ministry of Economy and Competitiveness, Institute of Health Carlos III (grant number PI14/00328), the Spanish Ministry of Science, Innovation and Universities (RTI2018–099200-B-I00), and the Generalitat of Catalonia, Agency for Management of University and Research Grants (2017SGR696) and Department of Health (SLT002/16/00250) to RP. This study has been co-financed by FEDER funds from the European Union (‘A way to build Europe’).

**Compliance with ethical standards**

**Conflict of interest** The authors declare that they have no conflict of interest.

## References

- Antikainen H, Driscoll M, Haspel G, Dobrowolski R. TOR-mediated regulation of metabolism in aging. *Aging Cell*. 2017;16:1219–33. <https://doi.org/10.1111/acel.12689>.
- Bárceña C, López-Otín C, Kroemer G. Methionine restriction for improving progeria: another autophagy-inducing anti-aging strategy? *Autophagy*. 2019;15:558–9. <https://doi.org/10.1080/15548627.2018.1533059>.
- Barja G. Mitochondrial free radical production and aging in mammals and birds. *Ann N Y Acad Sci*. 1998;854:224–38. <https://doi.org/10.1111/j.1749-6632.1998.tb09905.x>.
- Barja G. The gene cluster hypothesis of aging and longevity. *Biogerontology*. 2008;9:57–66. <https://doi.org/10.1007/s10522-007-9115-5>.
- Barja G. Longevity and evolution. New York: Nova Science Publishers, Inc.; 2010.
- Barja G. Towards a unified mechanistic theory of aging. *Exp Gerontol*. 2019;124:110627. <https://doi.org/10.1016/j.exger.2019.05.016>.
- Barja G, Cadenas S, Rojas C, Pérez-Campo R, López-Torres M. Low mitochondrial free radical production per unit O<sub>2</sub> consumption can explain the simultaneous presence of high longevity and high aerobic metabolic rate in birds. *Free Radic Res*. 1994;21:317–27. <https://doi.org/10.3109/10715769409056584>.
- Bowles JT. The evolution of aging: a new approach to an old problem of biology. *Med Hypotheses*. 1998;51:179–221. [https://doi.org/10.1016/S0306-9877\(98\)90079-2](https://doi.org/10.1016/S0306-9877(98)90079-2).
- Bozek K, Khrameeva EE, Reznick J, Omerbašić D, Bennett NC, Lewin GR, et al. Lipidome determinants of maximal lifespan in mammals. *Sci Rep*. 2017;7:1–5. <https://doi.org/10.1038/s41598-017-00037-7>.

- Cabr e R, Jov e M, Naud ı A, Ayala V, Pi nol-Ripoll G, Gil-Villar MP, et al. Specific metabolomics adaptations define a differential regional vulnerability in the adult human cerebral cortex. *Front Mol Neurosci*. 2016;9. <https://doi.org/10.3389/fnmol.2016.00138>.
- Caraveo G, Soste M, Cappelletti V, Fanning S, van Rossum DB, Whitesell L, et al. FKBP12 contributes to  $\alpha$ -synuclein toxicity by regulating the calcineurin-dependent phosphoproteome. *Proc Natl Acad Sci*. 2017;114:311–22. <https://doi.org/10.1073/pnas.1711926115>.
- Caron A, Richard D, Laplante M. The roles of mTOR complexes in lipid metabolism. *Annu Rev Nutr*. 2015;35:321–48. <https://doi.org/10.1146/annurev-nutr-071714-034355>.
- Chiang GG, Abraham RT. Phosphorylation of mammalian target of rapamycin (mTOR) at Ser-2448 is mediated by p70S6 kinase. *J Biol Chem*. 2005;280:25485–90. <https://doi.org/10.1074/jbc.M501707200>.
- Chong J, Wishart DS, Xia J. Using MetaboAnalyst 4.0 for comprehensive and integrative metabolomics data analysis. *Curr Protoc Bioinforma*. 2019;68. <https://doi.org/10.1002/cpbi.86>.
- Cooper N, Thomas GH, FitzJohn RG. Shedding light on the ‘dark side’ of phylogenetic comparative methods. *Methods Ecol Evol*. 2016;7:693–9. <https://doi.org/10.1111/2041-210X.12533>.
- Cunningham JT, Rodgers JT, Arlow DH, Vazquez F, Mootha VK, Puigserver P. mTOR controls mitochondrial oxidative function through a YY1–PGC-1 $\alpha$  transcriptional complex. *Nature*. 2007;450:736–40. <https://doi.org/10.1038/nature06322>.
- D uvel K, Yecies JL, Menon S, Raman P, Lipovsky AI, Souza AL, et al. Activation of a metabolic gene regulatory network downstream of mTOR complex 1. *Mol Cell*. 2010;39:171–83. <https://doi.org/10.1016/j.molcel.2010.06.022>.
- Figueiredo VC, Markworth JF, Cameron-Smith D. Considerations on mTOR regulation at serine 2448: implications for muscle metabolism studies. *Cell Mol Life Sci*. 2017;74:2537–45. <https://doi.org/10.1007/s00018-017-2481-5>.
- Fontana L, Partridge L, Longo VD. Extending healthy life span—from yeast to humans. *Science*. 2010;328(80):321–6. <https://doi.org/10.1126/science.1172539>.
- Fredslund J, Schauser L, Madsen LH, Sandal N, Stougaard J. PriFi: using a multiple alignment of related sequences to find primers for amplification of homologs. *Nucleic Acids Res*. 2005;33:516–20. <https://doi.org/10.1093/nar/gki425>.
- Fushan AA, Turanov AA, Lee S-G, Kim EB, Lobanov AV, Yim SH, et al. Gene expression defines natural changes in mammalian lifespan. *Aging Cell*. 2015;14:352–65. <https://doi.org/10.1111/acer.12283>.
- Gomez A, Gomez J, Torres ML, Naudi A, Mota-Martorell N, Pamplona R, et al. Cysteine dietary supplementation reverses the decrease in mitochondrial ROS production at complex I induced by methionine restriction. *J Bioenerg Biomembr*. 2015;47. <https://doi.org/10.1007/s10863-015-9608-x>.
- Gu X, Orozco JM, Saxton RA, et al. SAMTOR is an S-adenosylmethionine sensor for the mTORC1 pathway. *Science*. 2017;358(80):813–8. <https://doi.org/10.1126/science.aao3265>.
- Guarente L, Kenyon C. Genetic pathways that regulate ageing in model organisms. *Nature*. 2000;408:255–62. <https://doi.org/10.1038/35041700>.
- Hoeffler CA, Tang W, Wong H, Santillan A, Patterson RJ, Martinez LA, et al. Removal of FKBP12 enhances mTOR-Raptor interactions, LTP, memory, and perseverative/repetitive behavior. *Neuron*. 2008;60:832–45. <https://doi.org/10.1016/j.neuron.2008.09.037>.
- Jeon JS, Oh J-J, Kwak HC, Yun HY, Kim HC, Kim YM, et al. Age-related changes in sulfur amino acid metabolism in male C57BL/6 mice. *Biomol Ther (Seoul)*. 2018;26:167–74. <https://doi.org/10.4062/biomolther.2017.054>.
- Johnson SC, Rabinovitch PS, Kaeberlein M. mTOR is a key modulator of ageing and age-related disease. *Nature*. 2013;493:338–45. <https://doi.org/10.1038/nature11861>.
- Jones OR, Scheuerlein A, Salguero-G omez R, Camarda CG, Schaible R, Casper BB, et al. Diversity of ageing across the tree of life. *Nature*. 2014;505:169–73. <https://doi.org/10.1038/nature12789>.
- Jov e M, Naud ı A, Aledo JC, Cabr e R, Ayala V, Portero-Otin M, et al. Plasma long-chain free fatty acids predict mammalian longevity. *Sci Rep*. 2013;3:3346. <https://doi.org/10.1038/srep03346>.
- Kapahi P, Chen D, Rogers AN, Katewa SD, Li PWL, Thomas EL, et al. With TOR, less is more: a key role for the conserved nutrient-sensing TOR pathway in aging. *Cell Metab*. 2010;11:453–65. <https://doi.org/10.1016/j.cmet.2010.05.001>.
- Kenyon CJ. The genetics of ageing. *Nature*. 2010;464:504–12. <https://doi.org/10.1038/nature08980>.
- Kim EB, Fang X, Fushan AA, Huang Z, Lobanov AV, Han L, et al. Genome sequencing reveals insights into physiology and longevity of the naked mole rat. *Nature*. 2011;479:223–7. <https://doi.org/10.1038/nature10533>.
- Kumar S, Stecher G, Suleski M, Hedges SB. TimeTree: a resource for timelines, timetrees, and divergence times. *Mol Biol Evol*. 2017;34:1812–9. <https://doi.org/10.1093/molbev/msx116>.
- Lewis KN, Rubinstein ND, Buffenstein R. A window into extreme longevity; the circulating metabolomic signature of the naked mole-rat, a mammal that shows negligible senescence. *GeroScience*. 2018;40:105–21. <https://doi.org/10.1007/s11357-018-0014-2>.
- Libertini G. An adaptive theory of the increasing mortality with increasing chronological age in populations in the wild. *J Theor Biol*. 1988;132:145–62. [https://doi.org/10.1016/S0022-5193\(88\)80153-X](https://doi.org/10.1016/S0022-5193(88)80153-X).
- Liu Y, Song D, Xu B, Li H, Dai X, Chen B. Development of a matrix-based candidate reference material of total homocysteine in human serum. *Anal Bioanal Chem*. 2017;409:3329–35. <https://doi.org/10.1007/s00216-017-0272-3>.
- Longo VD, Mitteldorf J, Skulachev VP. Programmed and altruistic ageing. *Nat Rev Genet*. 2005;6:866–72. <https://doi.org/10.1038/nrg1706>.
- Longo VD, Antebi A, Bartke A, Barzilay N, Brown-Borg HM, Caruso C, et al. Interventions to slow aging in humans: are we ready? *Aging Cell*. 2015;14:497–510. <https://doi.org/10.1111/acer.12338>.

- Lushchak O, Strilbytska O, Piskovatska V, Storey KB, Koliada A, Vaiserman A. The role of the TOR pathway in mediating the link between nutrition and longevity. *Mech Ageing Dev.* 2017;164:127–38. <https://doi.org/10.1016/j.mad.2017.03.005>.
- Ma S, Gladyshev VN. Molecular signatures of longevity: insights from cross-species comparative studies. *Semin Cell Dev Biol.* 2017;70:190–203. <https://doi.org/10.1016/j.semcdb.2017.08.007>.
- Ma S, Yim SH, Lee S-G, Kim EB, Lee SR, Chang KT, et al. Organization of the mammalian metabolome according to organ function, lineage specialization and longevity. *Cell Metab.* 2015;22:332–43. <https://doi.org/10.1016/j.cmet.2015.07.005>.
- Ma S, Upneja A, Galecki A, Tsai YM, Burant CF, Raskind S, et al. Cell culture-based profiling across mammals reveals DNA repair and metabolism as determinants of species longevity. *Elife.* 2016;5:1–25. <https://doi.org/10.7554/eLife.19130>.
- Mitteldorf J. Aging is a group-selected adaptation: theory, evidence, and medical implications. Boca Raton: CRC Press; 2016.
- Mitteldorf J. Can aging be programmed? *Biochem.* 2018;83:1524–33. <https://doi.org/10.1134/S0006297918120106>.
- Miwa S, Jow H, Baty K, Johnson A, Czapiewski R, Saretzki G, et al. Low abundance of the matrix arm of complex I in mitochondria predicts longevity in mice. *Nat Commun.* 2014;5:1–12. <https://doi.org/10.1038/ncomms4837>.
- Mota-Martorell N, Pradas I, Jové M, Naudí A, Pamplona R. Biosíntesis de novo de glicerofosfolípidos y longevidad. *Rev Esp Geriatr Gerontol.* 2019;54:88–93. <https://doi.org/10.1016/j.regg.2018.05.006>.
- Muntané G, Farré X, Rodríguez JA, Pegueroles C, Hughes DA, de Magalhães JP, et al. Biological processes modulating longevity across primates: a phylogenetic genome-phenome analysis. *Mol Biol Evol.* 2018;35:1990–2004. <https://doi.org/10.1093/molbev/msy105>.
- Nascimento EBM, Snel M, Guigas B, van der Zon GCM, Kriek J, Maassen JA, et al. Phosphorylation of PRAS40 on Thr246 by PKB/AKT facilitates efficient phosphorylation of Ser183 by mTORC1. *Cell Signal.* 2010;22:961–7. <https://doi.org/10.1016/j.cellsig.2010.02.002>.
- Naudí A, Jové M, Ayala V, Portero-Otín M, Barja G, Pamplona R. Membrane lipid unsaturation as physiological adaptation to animal longevity. *Front Physiol.* 2013;4:372. <https://doi.org/10.3389/fphys.2013.00372>.
- Pamplona R, Barja G. Mitochondrial oxidative stress, aging and caloric restriction: the protein and methionine connection. *Biochim Biophys Acta Bioenerg.* 2006;1757:496–508. <https://doi.org/10.1016/j.bbabi.2006.01.009>.
- Pamplona R, Barja G. Highly resistant macromolecular components and low rate of generation of endogenous damage: two key traits of longevity. *Ageing Res Rev.* 2007;6:189–210. <https://doi.org/10.1016/j.arr.2007.06.002>.
- Pamplona R, Barja G. An evolutionary comparative scan for longevity-related oxidative stress resistance mechanisms in homeotherms. *Biogerontology.* 2011;12:409–35. <https://doi.org/10.1007/s10522-011-9348-1>.
- Pamplona R, Barja G, Portero-Otín M. Membrane fatty acid unsaturation, protection against oxidative stress and maximum life span. *Ann N Y Acad Sci.* 2002;959:475–90. <https://doi.org/10.1111/j.1749-6632.2002.tb02118.x>.
- Papadopoli D, Boulay K, Kazak L, et al. mTOR as a central regulator of lifespan and aging. *F1000Research.* 2019;8:998. <https://doi.org/10.12688/f1000research.17196.1>.
- Passtoors WM, Beekman M, Deelen J, van der Breggen R, Maier AB, Guigas B, et al. Gene expression analysis of mTOR pathway: association with human longevity. *Aging Cell.* 2013;12:24–31. <https://doi.org/10.1111/acer.12015>.
- Perez-Campo R, López-Torres M, Cadenas S, Rojas C, Barja G. The rate of free radical production as a determinant of the rate of aging: evidence from the comparative approach. *J Comp Physiol B Biochem Syst Environ Physiol.* 1998;168:149–58. <https://doi.org/10.1007/s003600050131>.
- Ruckenstuhl C, Netzerberger C, Entfellner I, Carmona-Gutierrez D, Kickenweiz T, Stekovic S, et al. Lifespan extension by methionine restriction requires autophagy-dependent vacuolar acidification. *PLoS Genet.* 2014;10:e1004347. <https://doi.org/10.1371/journal.pgen.1004347>.
- Sahm A, Bens M, Henning Y, et al. Higher gene expression stability during aging in long-lived giant mole-rats than in short-lived rats. *Aging (Albany NY).* 2018;10:3938–56. <https://doi.org/10.18632/aging.101683>.
- Sancak Y, Thoreen CC, Peterson TR, Lindquist RA, Kang SA, Spooner E, et al. PRAS40 is an insulin-regulated inhibitor of the mTORC1 protein kinase. *Mol Cell.* 2007;25:903–15. <https://doi.org/10.1016/j.molcel.2007.03.003>.
- Schieke SM, Phillips D, McCoy JP, et al. The mammalian target of rapamycin (mTOR) pathway regulates mitochondrial oxygen consumption and oxidative capacity. *J Biol Chem.* 2006;281:27643–52. <https://doi.org/10.1074/jbc.M603536200>.
- Selman C, Tullet JMA, Wieser D, et al. Ribosomal protein S6 kinase 1 signaling regulates mammalian life span. *Science.* 2009;326(80):140–4. <https://doi.org/10.1126/science.1177221>.
- Simonsen A, Cumming RC, Brech A, Isakson P, Schubert DR, Finley KD. Promoting basal levels of autophagy in the nervous system enhances longevity and oxidant resistance in adult *Drosophila*. *Autophagy.* 2008;4:176–84. <https://doi.org/10.4161/auto.5269>.
- Singh PP, Demmitt BA, Nath RD, Brunet A. The genetics of aging: a vertebrate perspective. *Cell.* 2019;177:200–20. <https://doi.org/10.1016/j.cell.2019.02.038>.
- Skulachev VP. Aging is a specific biological function rather than the result of a disorder in complex living systems: biochemical evidence in support of Weismann's hypothesis. *Biochemistry (Mosc).* 1997;62:1191–5.
- Tyshkovskiy A, Bozaykut P, Borodinova AA, et al. Identification and application of gene expression signatures associated with lifespan extension. *Cell Metab.* 2019;30:573–593.e8. <https://doi.org/10.1016/j.cmet.2019.06.018>.
- Valvezan AJ, Manning BD. Molecular logic of mTORC1 signaling as a metabolic rheostat. *Nat Metab.* 2019;1:321–33. <https://doi.org/10.1038/s42255-019-0038-7>.

Weichhart T. mTOR as regulator of lifespan, aging, and cellular senescence: a mini-review. *Gerontology*. 2018;64:127–34. <https://doi.org/10.1159/000484629>.

Wu JJ, Liu J, Chen EB, Wang JJ, Cao L, Narayan N, et al. Increased mammalian lifespan and a segmental and tissue-specific slowing of aging after genetic reduction of mTOR

expression. *Cell Rep*. 2013;4:913–20. <https://doi.org/10.1016/j.celrep.2013.07.030>.

**Publisher's note** Springer Nature remains neutral with regard to jurisdictional claims in published maps and institutional affiliations.